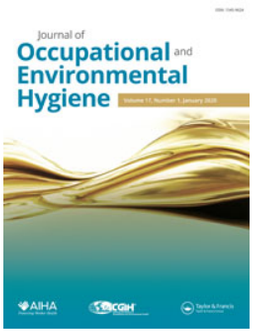

Journal of Occupational and Environmental Hygiene

ISSN: 1545-9624 (Print) 1545-9632 (Online) Journal homepage: https://www.tandfonline.com/loi/uoeh20

# Variability of aerosol mass and number concentrations during taconite mining operations

Nima Afshar-Mohajer, Rebecca Foos, John Volckens & Gurumurthy Ramachandran

**To cite this article:** Nima Afshar-Mohajer, Rebecca Foos, John Volckens & Gurumurthy Ramachandran (2020) Variability of aerosol mass and number concentrations during taconite mining operations, Journal of Occupational and Environmental Hygiene, 17:1, 1-14, DOI: 10.1080/15459624.2019.1688823

**To link to this article:** https://doi.org/10.1080/15459624.2019.1688823

Published online: 04 Dec 2019.

Submit your article to this journal

Article views: 431

View related articles

View Crossmark data

Citing articles: 5 View citing articles

Full Terms & Conditions of access and use can be found at
https://www.tandfonline.com/action/journalInformation?journalCode=uoeh20

JOURNAL OF OCCUPATIONAL AND ENVIRONMENTAL HYGIENE
2020, VOL. 17, NO. 1, 1–14
https://doi.org/10.1080/15459624.2019.1688823

Taylor & Francis
Taylor & Francis Group

Check for updates

# Variability of aerosol mass and number concentrations during taconite mining operations

Nima Afshar-Mohajer[a], Rebecca Foos[b], John Volckens[b], and Gurumurthy Ramachandran[a]

[a]Department of Environmental Health and Engineering, Johns Hopkins Bloomberg School of Public Health, Baltimore, Maryland, USA; [b]Department of Mechanical Engineering, Colorado State University, Fort Collins, Colorado, USA

**ABSTRACT**

This study characterized concentration metrics of airborne nanoparticles and their time series across major operations of a taconite mine through monitoring respirable and ultrafine particle concentrations at four major processing departments of the mine: crushing, dry milling, wet milling, and pelletizing (United Taconite Mine, Iron Junction, MN, USA). We used three area stations of direct-reading instruments to estimate concentration metrics including $PM_1$ (particles with an aerodynamic diameter $<1$ μm), respirable dust (particles sampled according to the respirable convention with a 50% sampling efficiency at an aerodynamic diameter of 4 μm), PN (total number concentration of particles), and lung-deposited surface area concentrations (LDSA) of particles smaller than 300 nm, on two different days. Results for each station were compared using bivariate correlation analysis to obtain insight into the spatial distribution, and intra-class correlation coefficients (ICCs) to evaluate the between-day repeatability between the measurements. Comparability of the LDSA concentrations measured by two different devices was also investigated using linear regression. Results revealed that the pelletizing operation produced the highest average LDSA concentration on both days (with a maximum concentration of $199 \pm 48$ $\mu m^2/cm^3$ in pelletizing, $141 \pm 52$ $\mu m^2/cm^3$ in crushing, $91 \pm 9$ $\mu m^2/cm^3$ in dry milling, and $85 \pm 7$ $\mu m^2/cm^3$ in wet milling). Concentrations in all operations showed a fair to excellent between-day repeatability but they were significantly different within stations of each operation. Measured LDSA concentrations did not show a linear correlation between different instruments, except for crushing.

**KEYWORDS**

Aerosol; crushing; DiSCmini; exposure; LDSA; milling; partector; pelletizing; UFP

## Introduction

Since late 1950s, the taconite mining industry in Minnesota has been the largest supplier of iron ore to the US steel industry. The dust generated during various processes in taconite mining is a well-recognized health hazard for taconite industry workers as it contains crystalline silica (Sheehy and McJilton 1987). In addition to cardiovascular and respiratory health issues resulting from occupational exposure to high concentrations of respirable particulate matter, crystalline silica found in taconite dust has been associated with silicosis and other fibrotic diseases (Nelson and Murray 2013). The Occupational Safety and Health Administration (OSHA) is currently in the midst of new proposed rule for controlling silica where workers' exposures would be limited to a new PEL of 50 micrograms of respirable crystalline silica per cubic meter of air ($\mu g/m^3$), averaged over an 8-hr day (Hwang et al. 2017).

The health impacts of exposure to airborne particulate matter (PM) generated in taconite mining processes have been investigated previously (Axten and Foster 2008; Clark et al. 1980; Higgins et al. 1983; Nolan et al. 1999). Most health studies on taconite mining and processing have focused on respirable dust (RD) concentration and elongate mineral particles (Nolan et al. 1999). However, many ore processing steps also generate large numbers of airborne ultrafine particles (UFP). These particles ($<100$ nm) contribute very little to the overall mass but dominate particle number concentrations and contribute substantially to total particle surface area. There is some evidence that particle number and surface area concentrations may be relevant metrics for health impact

CONTACT Gurumurthy Ramachandran gramach5@jhu.edu Department of Environmental Health and Engineering, Johns Hopkins Bloomberg School of Public Health, 615 N. Wolfe St., Baltimore, MD 21205.
Color versions of one or more of the figures in the article can be found online at www.tandfonline.com/uoeh.
© 2020 JOEH, LLC

assessment of exposure to UFP (Delfino et al. 2005; Park et al. 2010; Ramachandran et al. 2005). For instance, Lin et al. (2006) showed dose-dependent cytotoxicity of silica nanoparticles in human bronchoalveolar carcinoma-driven cells and their correlation to increased oxidative stress (Lin et al. 2006). Yu et al. (2009) demonstrated an increase in toxicity of the silica nanoparticles with a decrease in the particle size during in vivo exposure to mice.

Lung deposited surface area (LDSA) of nanoparticles has been hypothesized as a relevant dose metric of inhaled PM that explains 80% of the variability in acute lung inflammation (Schmid and Stoeger 2016). Use of LDSA concentration for dosimetry of the inhaled PM allows identification of material-based toxicity classes independent of particle size (Schmid et al. 2009). Measurements of the particle number concentration (PN) and its equivalent LDSA of the particles can be used to calculate the delivered dose of nanoparticles to the lungs of mine workers. In the case of PN, this is calculated as a product of the PN concentration and the volume of air breathed over a work-shift and the size-dependent lung deposition fractions in different regions of the respiratory tract. Since the LDSA already includes information about lung deposition patterns, the product of the LDSA concentration and the volume of air breathed over a work shift provides insight into occupational dose of PM smaller than 300 nm (Schmid et al. 2009; Kuhlbusch et al. 2011). Huynh et al. (2018) performed 4-hr sampling of submicron aerosol at area stations in taconite mines using direct-reading instruments to measure $PM_{2.5}$, PN, and LDSA in 91 locations across six mines located across the Mesabi Iron Range in northeastern Minnesota, USA. Their results indicated that concentrations of particles vary significantly at different times and locations.

Electrically charging nanoparticles with a unipolar diffusion charger has been the preferred technique for real-time detection of the LDSA concentration, especially for personal monitoring (Fissan et al. 2006). There are only a handful of these monitors commercially available including the Miniature Diffusion Size Classifier DiSCmini (Testo, Titisee-Neustadt, Germany) and the Partector (Naneos, Windisch, Switzerland) (Fierz et al. 2014). With a manufacturer recommended bias of ±30% for LDSA concentration estimation of nanoparticles between 20 and 400 nm, the DiSCmini and Partector have been recognized as convenient and relatively robust instruments for real-time detection of nanoparticles (Asbach et al. 2009; Todea et al. 2015). However, these monitors are subject to additional error when sampling hygroscopic particles or operate in high temperature/relative humidity environments. They also present different accuracies under low or high LDSA concentration and for small or large particle mode sizes. They also suffer from reduced counting efficiency for particle sizes below 20 nm. Moreover, their performance evaluation has been limited to controlled laboratory setup with no information when utilized in "real" industrial operations.

In this study, results of monitoring of several UFP concentration metrics at multiple area stations positioned in main operations of a taconite mine are presented. Recorded concentrations will help estimating the exposure of airborne fine and ultrafine PM inhaled by mine workers using mass-, number-, and surface-based PM exposure metrics in several operations during their work shift using real-time monitors. Between-day variability and inter-station comparisons of the concentration metrics within each process area along with comparability of the LDSA concentration measurements by DiSCmini monitors vs. Partector monitors are also investigated. For the first time, side-by-side comparison of the mentioned nano-aerosol monitors at a highly dusty site in an occupational setting is conducted.

## Methods

### *Mining processes*

All measurements reported in this study were obtained from a taconite mine in Northern Minnesota: United Taconite Mine, Iron Junction, MN, USA. After surface mining, the taconite ore undergoes four major processes in the following order: crushing, dry milling, wet milling, and pelletizing. Large ore-bearing rocks are delivered to the crushing department by trucks, then dumped into coarse primary crushers where they are reduced to sizes ~10 cm in diameter, and then to fine crushers where their sizes become as small as 1–2 cm. Ore dumping, and coarse and fine crushing, are all significant dust generating sources in the crushing operation. The crushed ore then undergoes a concentration process, where it is first dry milled, then mixed with water into a slurry and passed through a series of rod mills where it is converted into a sand-like consistency (wet milling). Magnetic separators then segregate the iron from the waste portion (so-called tailing) and concentrate the iron-bearing taconite grains. The water content is removed from slurry using disc filters. The filter cake is then mixed with a binding agent (bentonite) and

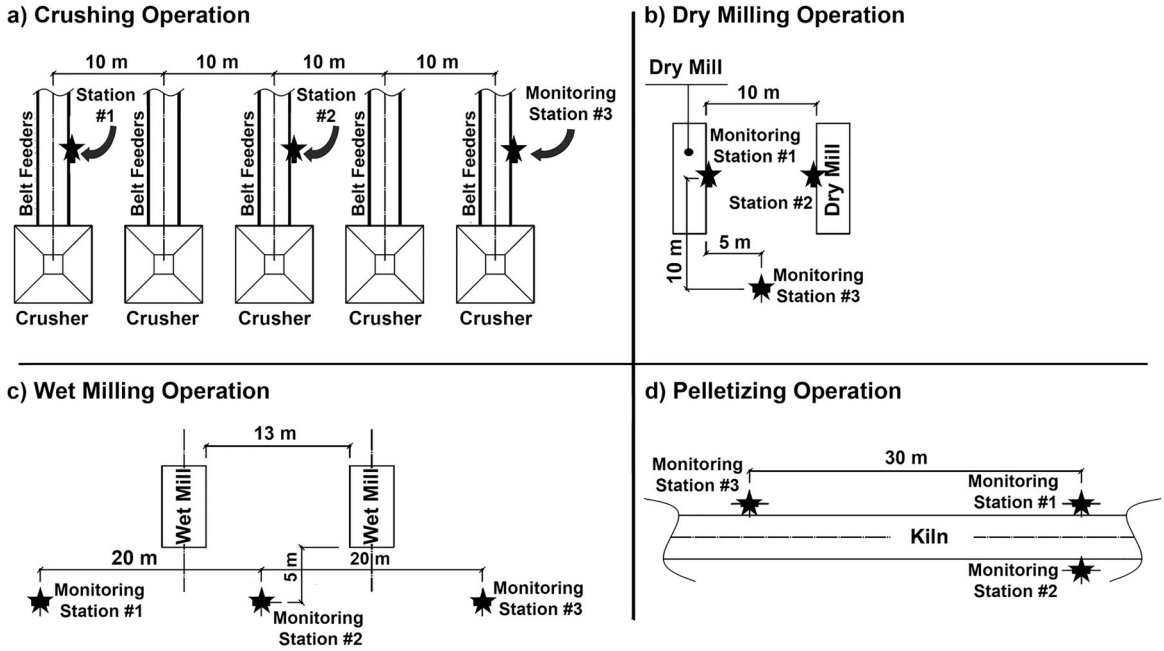


**Figure 1.** Approximate positioning of the sampling stations across each operation unit.

the mixture is then fed into large rotating drums, which tumble and roll the mixture into marble-size pellets approximately 1 cm in diameter (pelletizing). Finally, the pellets are kiln dried at 1300 °C for shipment to steel mills (McDonald et al. 2013).

### *Stations and aerosol monitoring procedure*

Measurements were made at three stations in each of the four departments (crushing, dry milling, wet milling, and pelletizing) on two randomly selected days. The reason for selecting random times for sampling was that each operation consisted of a series of activities performed continuously 24 hr a day and 7 days a week. The sampling period on Day 1 was in the afternoon and the sampling period on Day 2 was in the morning. The layout and distances between the sampling stations in each department are displayed in Figure 1. At each sampling station, multiple direct-reading instruments were located to measure the number, mass, and surface-area concentration of the particles. Particle mass concentrations for different size ranges (i.e., $PM_1$ and RD) were estimated by DustTrak aerosol monitors (Handheld DRX II Model 8532, TSI Inc., Shoreview, MN, USA), PNs and the particle mode sizes ($d_p$) were estimated by a DiSCmini nano-aerosol monitor (Testo, Titisee-Neustadt, Germany), and LDSAs were estimated by both a DiSCmini and a Partector nano-aerosol monitor (Naneos, Windisch, Switzerland). DustTrak aerosol monitors measure real-time mass concentrations using the relationship between scattered light intensity collected by a mirror from different angles in a detection chamber using a laser diode with a wavelength of 780 nm. These instruments utilize a sheath air system to protect the instrument optics and a laser photometer to estimate particle mass concentration. DustTrak monitors are ideal for estimating aerosol mass concentration in occupational settings as they cover a wide concentration range of 0.001–150 mg/m$^3$. However, recorded mass concentrations by the photometers depends on the size distribution of the aerosol and the optical properties (e.g., refractive index) of the particles that can lead to measured concentrations that are considerably different than the true concentrations (O'Shaughnessy et al. 2002). Therefore, integrated mass concentration of RD was estimated following method 0600 of the Manual of Analytical Methods by the National Institute of Occupational Safety and Health (NIOSH-NMAM 0600). Each DustTrak in a station was paired with an aluminum cyclone (Respirable Dust Aluminum Cyclone, SKC Inc., Eighty Four, PA, USA) running at a calibrated flow rate of 2.5 L/min and positioned vertically with a 37-mm PVC filter cassette to collect RD over the sampling period and gravimetric analysis was used to determine the average RD concentration. Then, all recorded concentrations for RD by DustTrak monitors were corrected by multiplying a correction factor (estimated to be 0.69) defined as the ratio of the average concentration from gravimetric analysis to the average concentration from DustTrak. This is in

addition to the internal correction done by the instrument itself. We assumed the same gravimetric correction factor obtained for RD for correcting recorded $PM_1$ concentrations by the DustTrak. Partector nano-aerosol monitors induce an electrical charge on surfaces of the sampled particles and subsequently detect the charged particles and determine their LDSA concentrations (Todea et al. 2015). The particle size range and the LDSA concentration range of Partector monitors are 10–400 nm and 0–20,000 $\mu m^2/cm^3$ respectively. Similar to Partector monitors, DiSCmini monitors apply corona charging to charge the particles and then estimate their LDSA concentrations. The DiSCmini nano-aerosol monitors measure the electric current resulting from the impact of charged particles onto stainless steel grids, followed by a high efficiency final filter to estimate PN and $d_p$ assuming a lognormal size distribution for airborne particles (Todea et al. 2015). The range of LDSA concentration by DiSCmini monitors is not reported, but the particle size range and PN concentration range of DiSCmini monitors are 10–700 nm and $10^3$–$10^6$ $\#/cm^3$, respectively.

The DustTrak, DiSCmini, and Partector logged data every second; all recorded concentration data were then averaged over 1-min intervals. The sampling time was at least 2.5 hr on each day of sampling. Data recorded by the DiSCmini and Partector were further corrected for temperature and relative humidity (RH) using correlations provided by the manufacturer. There was a slight difference between the monitoring instruments used in Station #3 compared to the other two stations. At Station #1 and #2, particle mass concentrations ($PM_1$ and RD) were estimated by a DustTrak aerosol detector, PNs and particle mode sizes were estimated by a DiSCmini nano-aerosol monitor, and LDSAs were estimated by both a DiSCmini and a Partector nano-aerosol. Station #3 included only one DiSCmini and one Partector nano-aerosol monitor (no DustTrak) and therefore only obtained particle mode sizes, PN, and LDSA concentrations.

## Statistical analysis of the data

### Inter-comparison of the stations within a department

Inter-comparison of the readings across different stations within a department recorded by the same type of monitoring instrument provides insight into uniformity of the concentration metrics at a certain time in an operation. For this purpose, bivariate correlation analysis similar to Garcia et al. (2013) was conducted by calculating the Spearman correlation factor for each concentration metric. While autocorrelation between measurements at consecutive time points is commonly seen when analyzing time-series data and needs to be adjusted for when estimating or comparing exposure estimates, autocorrelation between measurements of the same concentration metric at different stations is not expected. Therefore, we did not adjust analyses for autocorrelation. Each run compared two stations at a time (Station #1 vs. Station #2, Station #2 vs. Station #3, and Station #3 vs. Station #1) to investigate the degree of correlation. All concentration values obtained over 2.5 hr of sampling were included in the model (sample size N = 150 for 150 min).

### Between-day correlation

Correlation between concentration values from one day to the next for routine operations was investigated following intra-class correlation (ICC) (Todea et al. 2015). The ICC is derived from the analysis of variance and estimates the percentage of the data points that reliably remain unchanged across different measurement times (Bartko 1966). Measurements of $PM_1$, RD, LDSA, PN, and $d_p$ during the sampling period of Day 1 were compared to the measured values by the same monitor in the same station during the sampling period of Day 2. Since taconite mining operations include multiple periodic activities occurring continuously, the same range of values (repeated periodically) is expected for each concentration metric recorded by a monitor. Therefore, ICC calculation of each concentration metric in a station required sorting the concentration values from the lowest to the highest before inputting into the model (a sample size of N = 150 for 150 min of the sampling period). The ICC of each concentration metric ranged from 0–1 and indicated the probability of having the same value for that concentration metric (no change in concentration at ICC = 1). For all ICCs, a confidence interval of 95% was considered. Since each set of compared data were recorded by the same data-logging device, a two-way mixed-effect model type of the ICC (so-called ICC(3,1)), as described by Shrout and Fleiss (1979), was used for the analysis. The ICCs estimated in this study are frequently used when the focus is on the repeatability of the measurements by the same monitor over different times. The formulation for estimation of the ICCs obtained in this study is given by Equation (1):

$$ICC(3,1) = \frac{MS_B - MS_E}{MS_B + (k-1)MS_E}, \qquad (1)$$

where $MS_B$ is the between-day mean squares of values of a concentration metric and $MS_E$ is the within-day mean squares of values of a concentration metric and $k$ is the number of concentration metric entries per day of sampling. Statistical analysis for calculation of the ICC values then was performed using SPSS® ver. 21 (IBM Analytics Inc., Armonk, NY, USA).

### Comparability of the LDSA measured by Partector and DiSCmini

Neither the Partector nor the DiSCmini is considered a reference instrument. Since both instruments are subject to measurement errors, an orthogonal regression analysis was used to compare the LDSA concentrations measured by Partectors vs. those by DiSCminis (Zellweger et al. 2009). This analysis was performed separately for each operation. All recorded LDSA concentrations by the three stations were included in the analysis. The slope and intercept estimates, associated $r^2$, and $p$-values of the relationship between the LDSA concentrations were calculated. This relationship should ideally be linear.

## Results

### Average concentrations

The time series of the concentration metrics measured by each monitor during crushing are displayed in Figure 2. The average baseline concentration of $PM_1$ in crushing operation was $157 \pm 24$ μg/m$^3$ on Day 1 and $130 \pm 9$ μg/m$^3$ on Day 2. On Day 1 of the crushing operation, $PM_1$ generally varied between 130 and 250 μg/m$^3$ with a spike at the 63rd min (~3:23 pm). However, fluctuations in the $PM_1$ time series on Day 2 showed a pronounced peak. On both days, concentrations measured by the monitors at all three stations followed the same rise and fall pattern, although the peaks in the PN and LDSA plots on Day 2 for Station #2 and Station #3 appeared with about a 25-min delay with respect to Day 1. On both days of sampling in crushing operation, the LDSA concentrations measured by the DiSCmini monitors were notably higher than those by the Partector monitors. In the crushing processes, the particle mode sizes varied considerably across days and stations. For instance, on Day 1, the average particle mode size was $36 \pm 15$ nm at Station #1 and increased to a maximum of 74 nm but on Day 2 at the same station, the average particle mode size was $29 \pm 28$ nm and increased to a maximum of 139 nm. The increase in both the total number concentration of particles and the particle mode size from 11:35 am to 12:15 pm on Day 2 might lead to the observed peak in the time series of $PM_1$ and RD concentrations.

The time series of the dry milling operation presented the least temporal variability across all the operations (see Figure 3). On Day 1, the average concentrations of $PM_1$ in dry milling operation was $96 \pm 8$ μg/m$^3$ at Station #1 and $90 \pm 7$ μg/m$^3$ at Station #2. Although $PM_1$ and RD concentrations in both stations were similar on Day 1, the averaged LDSA concentration and particle mode size at Station #2 were considerably lower than the other two stations (the average LDSA measured by Partector was 87 μm$^2$/cm$^3$ at Station #1, 58 μm$^2$/cm$^3$ at Station #2, and 93 μm$^2$/cm$^3$ at Station #3). The average particle mode size in all three stations of the dry milling operation was the lowest across all operations. On Day 2, the average concentration of $PM_1$ at Station #1 increased from $96 \pm 8$ to $106 \pm 9$ μg/m$^3$. In contrast to Day 1, the LDSA concentrations measured by both Partector and DiSCmini in all stations were comparable. An average increase in the total PN and decrease in the particle mode size on Day 2 compared to Day 1 in all stations implied occasional generation of particles smaller than 20 nm during dry milling.

On Day 1 of the wet milling operation, $PM_1$ and RD concentrations were significantly greater at Station #2 (Figure 4). Similar to the dry milling operation, there were minor fluctuations in the concentration metrics with no notable spikes and the particle mode size did not exceed 20 nm. Likewise, the average LDSA concentrations during wet milling operation was similar to those during dry milling operation. On Day 2, there were no significant differences between $PM_1$ and RD concentrations measured at Station #1 and #2.

The highest values of the concentration metrics were seen in the pelletizing operation. As seen in Figure 5, the time-series concentration plots of the pelletizing operation showed multiple peaks during sampling periods of both days. The average $PM_1$ concentrations measured by the DustTrak monitors of Station #1 and Station #2 were $168 \pm 4$ μg/m$^3$ and $169 \pm 4$ μg/m$^3$ on Day 1 and $195 \pm 4$ μg/m$^3$ and $192 \pm 3$ μg/m$^3$ on Day 2. The concentrations across different stations did not vary substantially. The average particle mode sizes across all stations in pelletizing operation were $19 \pm 2$ nm on Day 1 and $18 \pm 2$ nm on Day 2, which were larger than those of dry milling ($16 \pm 1$, $16 \pm 1$, and $17 \pm 1$ nm on Day 1 and $13 \pm 2$, $13 \pm 1$, and $12 \pm 1$ nm on Day 2) and wet milling operations ($16 \pm 1$, $16 \pm 1$, and $17 \pm 1$ nm on Day 1 and

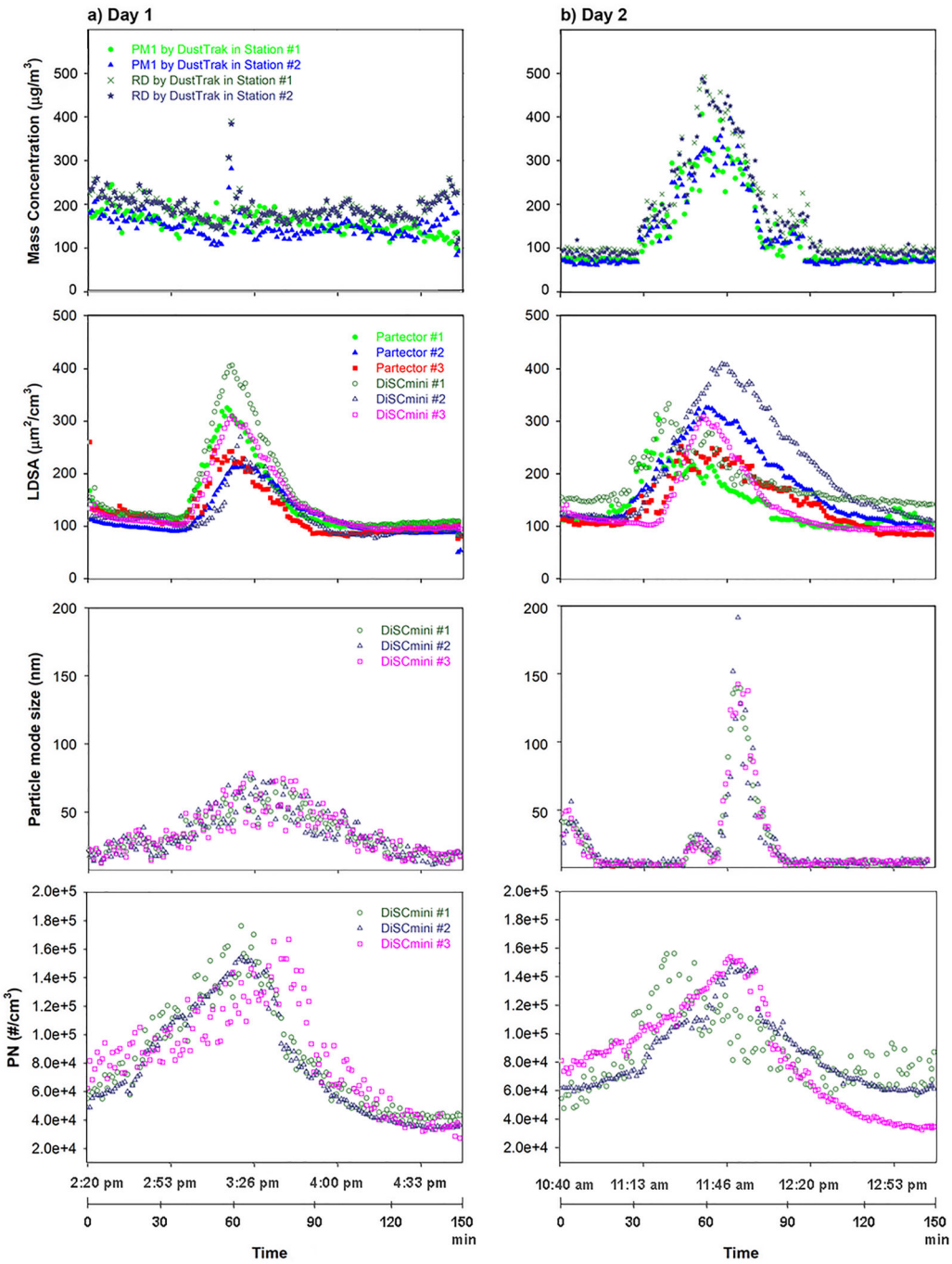


**Figure 2.** Time series of the aerosol concentrations ($PM_1$, RD, PN, LDSA) and particle mode sizes during crushing operation.

13 ± 2, 12 ± 1, and 13 ± 1 nm on Day 2), but much smaller than those observed in crushing operation (36 ± 15, 36 ± 17, and 36 ± 16 nm on Day 1 and 29 ± 28, 29 ± 28, and 30 ± 29 nm on Day 2).

### *Inter-comparison of the stations*

The Spearman correlation coefficient of each concentration metric of a mining operation is displayed in Figure 6. When comparing pairs of stations on each day, crushing operation was the only operation wherein all Spearman correlation coefficients (N = 150) of the concentration metrics were positive indicating that the directional change (increase or decrease in concentration of each metric) between each pair of stations was the same. Since Station #3 did not include a DustTrak monitor, concentration metrics of $PM_1$ and RD could only be compared

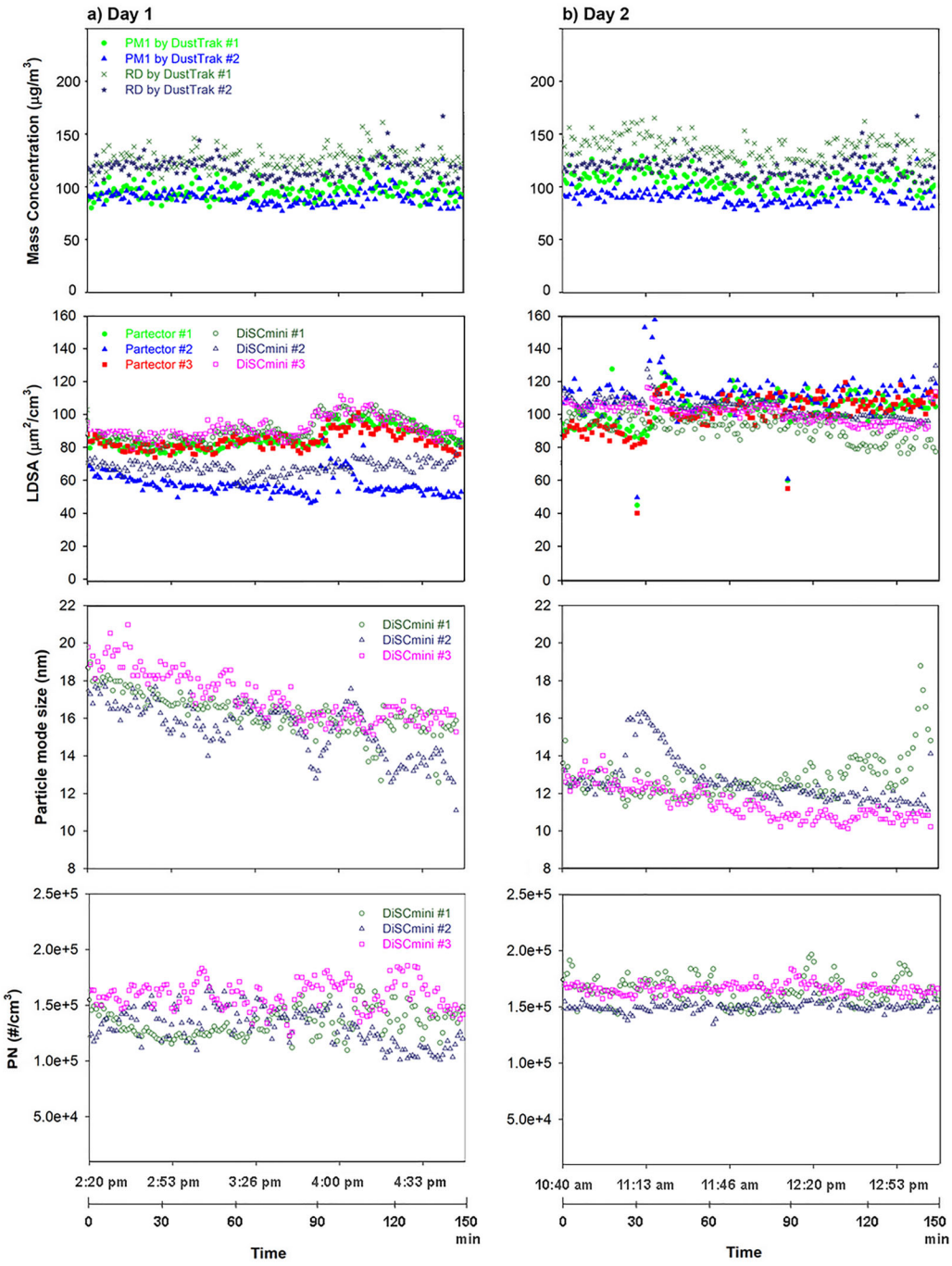


**Figure 3.** Time series of the aerosol concentrations ($PM_1$, RD, PN, LDSA) and particle mode sizes during dry milling operation.

between station #1 and #2. As seen in Figure 6, except for $PM_1$, all concentration metrics of the crushing operation had a correlation coefficient greater than 0.5. Also, crushing was the only operation wherein a PN correlation above 0.4 was observed. Except across stations of the pelletizing operation, the correlation coefficient of particle mode size was also greater than 0.5 on both days and all operations. Based on the results, the greatest correlation among the concentration metrics was seen in the crushing operation. No significant difference in Spearman correlation coefficient of Day 1 vs. Day 2 was observed.

### *Between-day repeatability correlations*

ICCs averaged across all stations of each operation (N = 150) are summarized in Table 1. Except for $PM_1$ and RD in crushing operation, all ICCs were greater than 0.75. Also, crushing was the only operation where the ICC value of LDSA measured by Partector

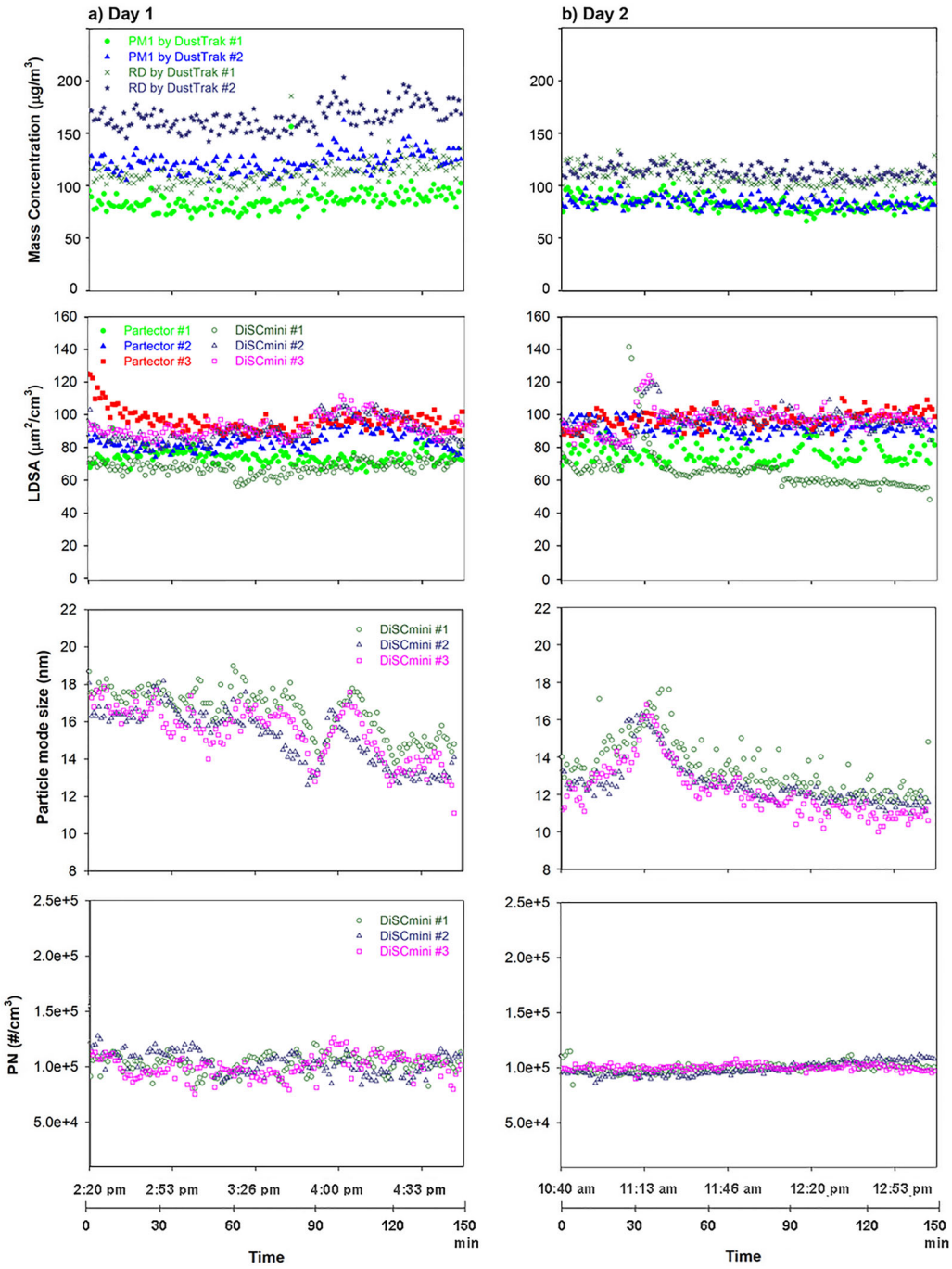


**Figure 4.** Time series of the aerosol concentrations ($PM_1$, RD, PN, LDSA) and particle mode sizes during wet milling operation.

was greater than that of measured by DiSCmini. Concentrations of PN showed a higher repeatability in crushing and pelletizing operations (average ICC of 0.97 and 0.99) compared to dry and wet milling (average ICC of 0.78 and 0.75). Particle mode size was the only metric with an ICC > 0.94 in all operations. One should note that the ICC values were averaged over all stations for each concentration metric. As seen in Table 1, no considerable change in ICC values of different stations within an operation was observed.

### *Comparability of the DiSCmini and Partector measurements*

The results of the linear regression analysis are summarized in Table 2. Estimated $r^2$s indicated that crushing operation was the only operation in which the linear relationship between the LDSA concentrations of DiSCmini and Partector monitors were highly correlated on both days ($r^2 = 0.97, 0.84, 0.80$ on Day 1 and $r^2 = 0.80, 0.89, 0.77$ on Day 2).

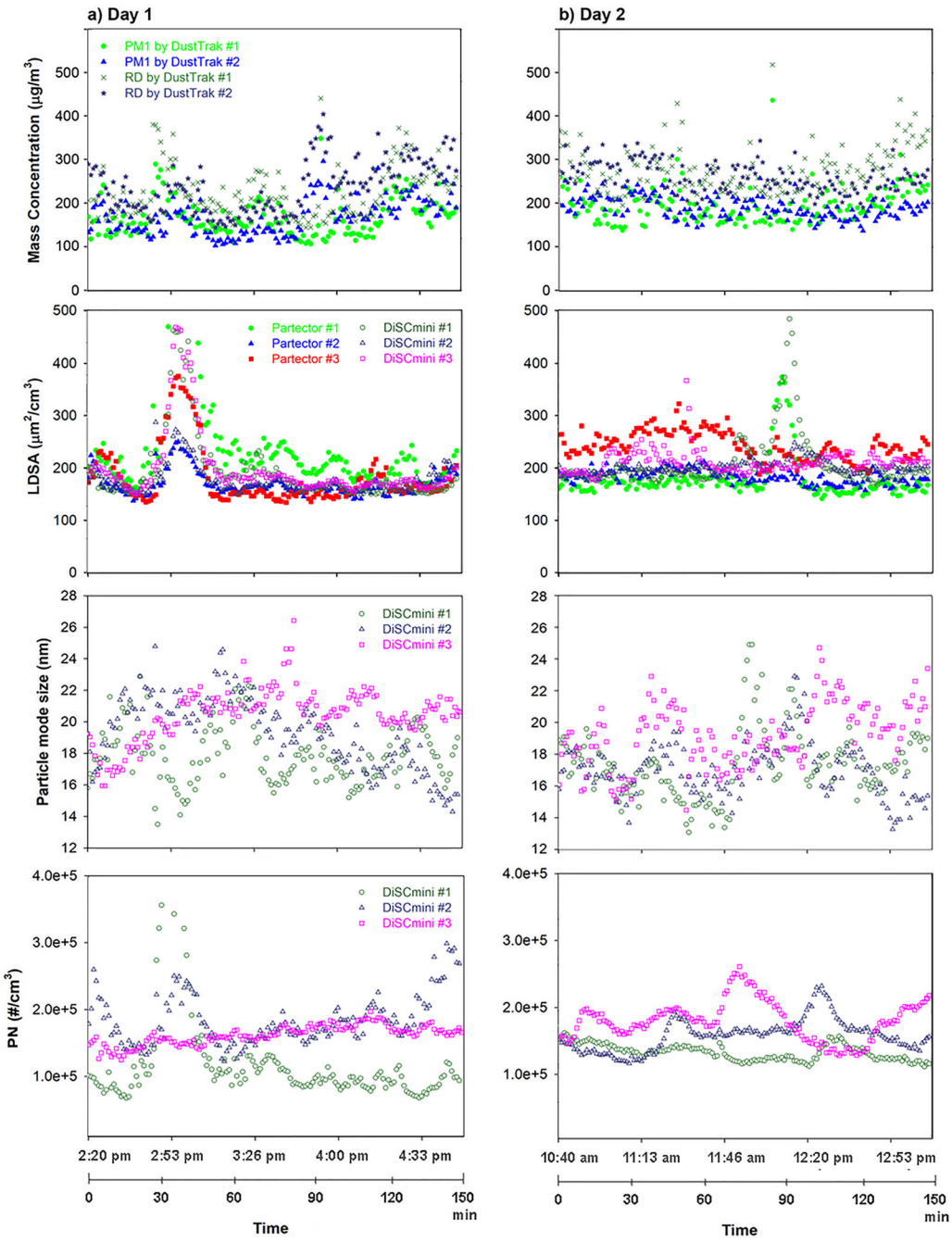


**Figure 5.** Time series of the aerosol concentrations ($PM_1$, RD, PN, LDSA) and particle mode sizes during pelletizing operation.

## Discussion

The time-series trends of the concentration metrics in crushing and pelletizing operations were similar. The times-series trends of the concentration metrics in dry milling and wet milling were comparable In crushing and pelletizing, the time series demonstrated one or two spikes considerably higher than the baseline concentration in all plots (on both days) but in milling operations (dry and wet), the concentration metrics were relatively steady throughout the course of sampling. Based on the particle mode diameter plots displayed in Figures 2–5, the majority of aerosolized nanoparticles were smaller than 75 nm (<25 nm if excluding crusher). This size range refers to UFP and corresponds to nucleation modes of aerosol formation. In the absence of chemical reactions, nucleation, coagulation, and condensation processes likely are forming the nano-sized particles. Specifically, the high temperature due to kiln operation in pelletizing operation (causing nucleation/condensation), inefficient

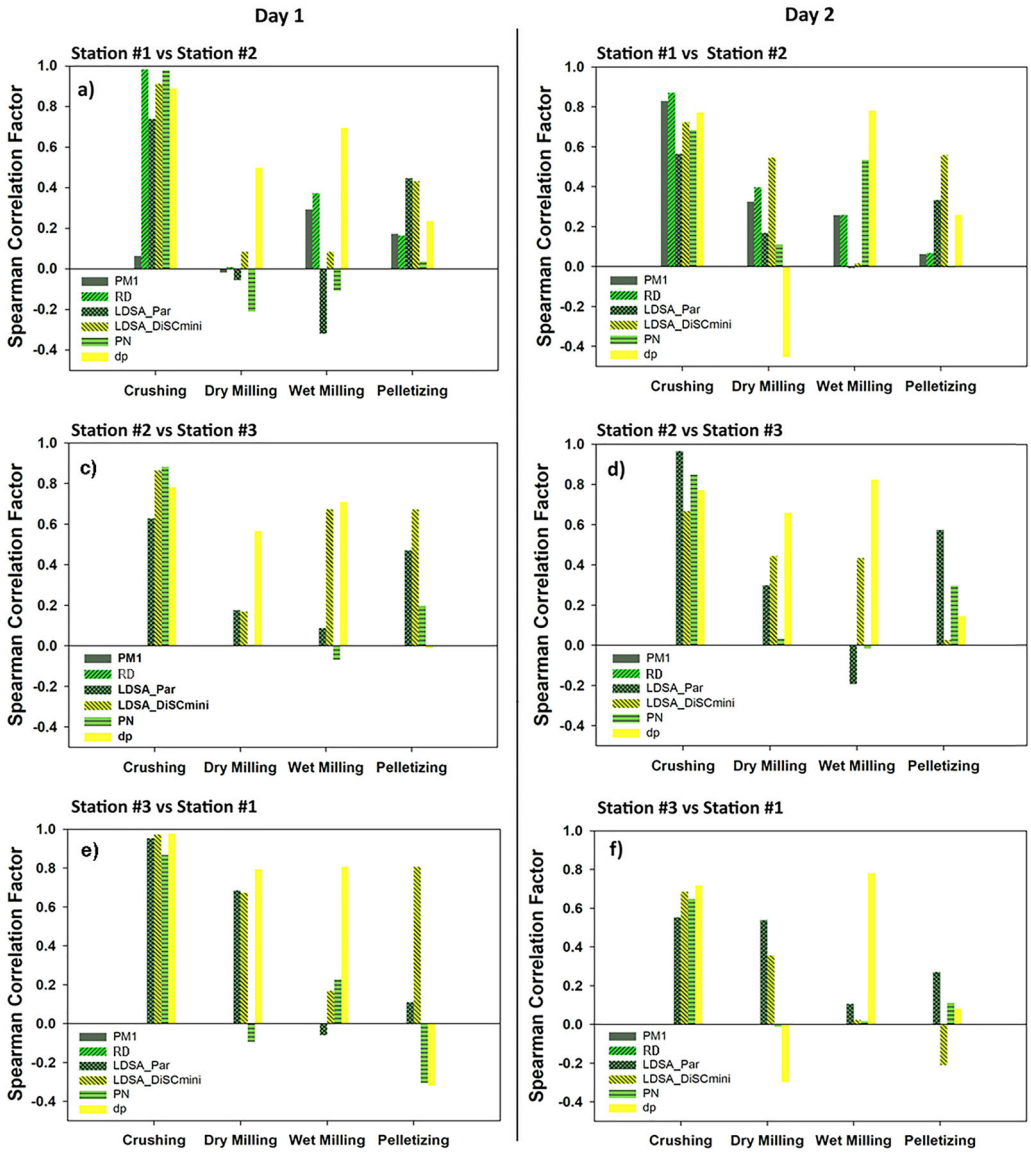


**Figure 6.** Spearman correlation factors for the inter-station comparisons of the aerosol concentration metrics: a) Station #1 vs. Station #2 on Day 1; b) Station #1 vs. Station #2 on Day 2; c) Station #2 vs. Station #3 on Day 1; d) Station #2 vs. Station #3 on Day 2; e) Station #3 vs. Station #1 on Day 1; and f) Station #3 vs. Station #1 on Day 2.

**Table 1.** Average between-day ICCs for different operations.

| Operation | $PM_1$* | Respirable Dust* | PN** | $d_p$** | LDSA by Partector** | LDSA by DiSCmini** |
|---|---|---|---|---|---|---|
| Crushing | 0.63 | 0.62 | 0.97 | 0.94 | 0.94 | 0.85 |
| Dry Milling | 0.99 | 0.99 | 0.78 | 0.99 | 0.83 | 0.93 |
| Wet Milling | 0.92 | 0.92 | 0.74 | 0.99 | 0.94 | 0.99 |
| Pelletizing | 0.99 | 0.99 | 0.99 | 0.99 | 0.80 | 0.92 |

*Between-day repeatability of the average values from Station #1 and #2
**Between-day repeatability of the average values from Station #1, #2, and #3

ventilation in all operations, and transport of nanoparticles from other processes into a target operation could be reasons for the relatively high LDSA concentrations. On average (over both days), the LDSA concentrations observed in crushing and pelletizing operations using Partector monitors were $142 \pm 52$ $\mu m^2/cm^3$ and $200 \pm 48$ $\mu m^2/cm^3$, which are comparable to the LDSA levels in a tungsten arc welding workshop: 137 $\mu m^2/cm^3$ as estimated by Geiss et al. (2016) using Partectors 2-m away from the welding electrodes.[26] The average LDSA concentrations in dry milling and wet milling were about half of those in crushing and pelletizing operations. The LDSA concentration range in milling operations is comparable to those generated by a fused

**Table 2.** Results of the orthogonal regression analysis on the LDSA concentrations ($y = ax + b$) between measurements by Partector and DiSCmini on each day of different operations (where x refers to Partector measurements and y refers to DiSCmini measurements).

| | Day 1 | | | Day 2 | | |
|---|---|---|---|---|---|---|
| Operation | Slope | Intercept ($\mu m^2/cm^3$) | $r^2$ | Slope | Intercept ($\mu m^2/cm^3$) | $r^2$ |
| **Crushing** | | | | | | |
| Station #1 | 1.36 ± 0.02 | −33.94 ± 3.13 | 0.97 | 0.94 ± 0.04 | 50.47 ± 5.72 | 0.80 |
| Station #2 | 0.93 ± 0.03 | 8.52 ± 4.11 | 0.84 | 1.27 ± 0.04 | −14.71 ± 6.99 | 0.89 |
| Station #3 | 1.24 ± 0.05 | −13.60 ± 6.61 | 0.80 | 1.05 ± 0.05 | −10.47 ± 7.18 | 0.77 |
| **Dry Milling** | | | | | | |
| Station #1 | 0.79 ± 0.07 | 22.89 ± 5.79 | 0.48 | −0.16 ± 0.05 | 109.28 ± 5.559 | 0.05 |
| Station #2 | 0.03 ± 0.05 | 66.80 ± 3.15 | 0.03 | 0.14 ± 0.03 | 88.90 ± 3.91 | 0.10 |
| Station #3 | 0.626 ± 0.08 | 39.69 ± 6.53 | 0.31 | −0.18 ± 0.04 | 117.93 ± 3.92 | 0.13 |
| **Wet Milling** | | | | | | |
| Station #1 | −0.02 ± 0.09 | 70.25 ± 6.47 | 0.01 | −0.20 ± 0.16 | 82.59 ± 12.30 | 0.04 |
| Station #2 | 0.93 ± 0.07 | 11.86 ± 5.86 | 0.55 | −0.45 ± 0.15 | 138.73 ± 13.87 | 0.05 |
| Station #3 | 0.02 ± 0.07 | 90.94 ± 7.26 | −0.01 | 0.23 ± 0.12 | 74.87 ± 12.12 | 0.02 |
| **Pelletizing** | | | | | | |
| Station #1 | 0.49 ± 0.01 | 70.51 ± 3.32 | 0.92 | 1.02 ± 0.06 | 27.14 ± 11.13 | 0.65 |
| Station #2 | 1.05 ± 0.03 | −1.14 ± 5.06 | 0.89 | 0.44 ± 0.08 | 119.51 ± 14.03 | 0.18 |
| Station #3 | 0.67 ± 0.03 | 61.14 ± 6.18 | 0.74 | 0.37 ± 0.06 | 121.37 ± 14.22 | 0.20 |

deposition modeling 3D printer that is heating up acrylonitrile butadiene styrene and operates in a 30-$m^3$ chamber: 67 $\mu m^2/cm^3$ (Geiss et al. 2016). This is particularly important as the same amount of RD may provide 10-fold increase in harmful health effects presuming the LDSA concentration to be a more relevant metric (Kuuluvainen et al. 2016).

A previous study by Huynh et al. (2018) showed that the average concentrations of RD for all similar exposure groups within crushing, dry milling, wet milling, and pelletizing were lower than the respirable dust (RD) threshold limit value (TLV®-TWA) regulated by the American Conference of Governmental Industrial Hygienists (ACGIH®) of 3 $mg/m^3$. According to their findings, there were an average RD of 70–185 $\mu g/m^3$ related to miners working in the crushing, an average RD of 108–256 $\mu g/m^3$ related to miners working in the concentrating (dry and wet milling altogether), and an average RD of 167–380 $\mu g/m^3$ related to miners working in the pelletizing department. The average RD concentrations measured in the present study across all stations and over two days were 179 $\mu g/m^3$ in crushing, 125 $\mu g/m^3$ in dry milling, 126 $\mu g/m^3$ in wet milling, and 251 $\mu g/m^3$ in pelletizing, which are all within the range reported by Huynh et al. (2018) during area monitoring. The sampling stations of crushing and wet milling were positioned as a horizontal line on the mine site layout. In the crushing operation, concentration metrics of the particles from one side to the other side of the sampled line showed a high correlation (Spearman coefficient >0.6 (except for $PM_1$) on both days, as seen in Figure 6a–f). On Day 1, only particle mode size showed a correlation greater than 0.6 in the wet and dry milling operations. On Day 2, particle mode size had a correlation greater than 0.6 only in the wet milling operation. PN concentrations of all operations except crushing indicated a high inter-station variability (Spearman correlation coefficient <0.2). Opposite to crushing and wet milling operation, the sampling stations for dry milling and pelletizing formed a triangle on the site layout that may have contributed in observing lower correlation factors in these operations compared to crushing and wet milling operations.

All ICCs listed in Table 1 were >0.62 indicating repeatability percentages greater than those Garcia et al. (2013) observed in personal monitoring of $PM_{2.5}$ and inhalable PM in the dairy industry. However, the between-day repeatability percentages of the concentration metrics were lower than those for concentrations of airborne spores and pollen with median diameters >2 μm, which are above 0.94 (Mitakakis et al. 2000). One should note that the excellent temporal repeatability of the concentration metrics discussed in the present study refers to the measured range of the concentrations as a whole—not repeatability of the data at a certain time or for a certain concentration.

Both Partector and DiSCmini are among the most common newer devices used for measurement of the airborne nanoparticles and both operate based on diffusion charging mechanism (Asbach et al. 2017). Also, both the DiSCmini and Partector provided comparable measurements for UFP monitoring. However, the relationship between the recorded concentrations were not linearly correlated in most cases. Except in crushing operation, the LDSA concentrations measured by the Partector monitors at a given time were slightly

greater than those measured by the DiSCmini monitors and the relationships had low $r^2$ (<0.65) to be linear.

Accuracy of the LDSA concentrations when measured by a DiSCmini has been investigated by Mills et al. (2013). They showed that the LDSA concentration of polydisperse aerosols of sodium chloride and metals estimated by the DiSCmini were 96–155% of those measured by a scanning mobility particle sizer (SMPS, TSI Inc., Shoreview, MN, USA), which indicated a tendency for overestimation. The weak linear correlation between Partector and DiSCmini concentrations resulted in the operations (except in crushing operation) in the current study may be due to sensitivity of these devices to low temperatures (<−15 °C on both days of sampling and high humidity (snowy days with relative humidity above 75% in wet milling). In the crushing operation with relatively larger nanoparticles (particle mode size larger than 20 nm at all times) compared to the other operations the strongest linearity between the LDSA concentrations was observed. However, a series of mechanical processes occurring in a taconite mine led to high concentrations of >400 nm particles, which are known responsible for significant biases in Partectors and DiSCminis (Todea et al. 2017). The linear relationship between these two instruments in crushing operation resulted in biases ranging from −7% to +36%. This range is in an agreement with findings of a study by Todea et al. (2015) wherein the researchers performed an inter-comparison chamber study with 29 different polydisperse test aerosols to a Partector and a DiSCmini and observed ±30% bias respect to the reference value obtained from a scanning mobility particle sizer (Todea et al. 2015). Accuracy determination of the monitors in their study was based on comparisons with a reference instrument—a scanning mobility particle sizer (SMPS Model 3936, TSI Inc., Shoreview, MN, USA). Comparative laboratory measurements by Todea et al. (2017) showed both DiSCmini and Partector monitors present similar underestimation or overestimation trends with respect to the true LDSA concentrations during co-located sampling. They also showed that for all tested cases concentrations varied from 1 to $24 \times 10^4$ #/cm$^3$ and $10 < d_p < 400$ nm, and the measured LDSA concentrations recorded by both monitors were within the manufacturer recommended bias of ±30%. Todea et al. (2017) reported an underestimated LDSA concentration in all cases by both monitors though the underestimating bias is below -30%. However, they concluded that both monitors present a greater accuracy (lower bias) with a decrease in true concentration as well as a greater accuracy with a decrease in $d_p$ (Todea et al. 2017). In the present study, the average values of LDSA and PN concentrations and $d_p$ were the lowest in milling operations. In absence of a reference instrument to measure LDSA or PN concentrations in the present work, findings by Todea et al. implied that DiSCmini and Partectors implemented in dry and wet milling operations might have a greater accuracy than those in crushing and pelletizing operations. One should note that the LDSA values applied into the orthogonal regression analysis might be autocorrelated and therefore the $r^2$ values may be affected by autocorrelation.

## Conclusions

Concentration metrics of airborne fine and ultrafine particles in a taconite mine site ($PM_1$, PN, LDSA, particle mode size) reported the highest average levels of $PM_1 = 200 \pm 48$ μg/m$^3$, $LDSA = 181 \pm 37$ μm$^2$/cm$^3$, and $PN = 1.57 \times 10^5$ #/cm$^3$ all in the pelletizing department. The wet milling operation presented the lowest LDSA and PN concentrations among the operations. The concentration metrics did not show a conclusive spatial trend but showed a temporal repeatability >62%, which is greater than the corresponding temporal repeatability percentages found in other occupational settings. The particle mode size of generated nanoparticles was finer than 25 nm in milling and pelletizing operations but were consistently larger than 30 nm in crushing operation. Partector and DiSCmini nanoparticle monitors were only linearly correlated in crushing operation ($r^2 > 0.8$) and one day pelletizing operation ($r^2 > 0.74$). The air monitoring results identified taconite operations with higher levels of exposure to UFP (pelletizing and crushing) and showed the variability of the concentrations and their increasing/decreasing trends which could help with development of non-engineering administrative controls to mitigate exposure of the workers.

## Acknowledgments

This research was funded by the National Institute of Occupational Safety and Health (Grant No. OH010662). Its contents are solely the responsibility of the authors and do not necessarily represent the official views of the Centers for Disease Control and Prevention or the Department of Health and Human Services. Authors are thankful to Mr. Karl Braun from Cleveland-Cliffs Inc. for his insightful consultation and assistance in the data collection. Authors are grateful to Dr. Tran Huynh and Dr. Harrison Quick for their insights regarding the statistical analyses.

## Disclaimer

The authors deny any conflict of interest in the present study.

## Funding

This research was funded by the National Institute of Occupational Safety and Health (Grant No. OH010662).

## ORCID

Nima Afshar-Mohajer http://orcid.org/0000-0002-6337-1824
John Volckens http://orcid.org/0000-0002-7563-9525

## References

**Asbach C, Alexander C, Clavaguera S, Dahmann D, Dozol H, Faure B, Fierz M, Fontana L, Iavicoli I, Kaminski H, MacCalman L**. 2017. Review of measurement techniques and methods for assessing personal exposure to airborne nanomaterials in workplaces. Sci Total Environ. 15(603):793–806. doi:10.1016/j.scitotenv.2017.03.049

**Asbach C, Kaminski H, Fissan H, Monz C, Dahmann D, Mülhopt S, Paur HR, Kiesling HJ, Herrmann F, Voetz M, Kuhlbusch TA**. 2009. Comparison of four mobility particle sizers with different time resolution for stationary exposure measurements. J Nanopart Res 11(7):1593. doi:10.1007/s11051-009-9679-x

**Axten CW, Foster D**. 2008. Analysis of airborne and waterborne particles around a taconite ore processing facility. Regul Toxicol Pharm. 52(1 Suppl.). doi:10.1016/j.yrtph.2007.11.010

**Bartko JJ**. 1966. The intraclass correlation coefficient as a measure of reliability. Psychol Rep. 19(1):3–11. doi:10.2466/pr0.1966.19.1.3

**Clark TC, Harrington VA, Asta J, Morgan WK, Sargent EN**. 1980. Respiratory effects of exposure to dust in taconite mining and processing. Am Rev Respir Dis. 121(6):959–966. doi:10.1164/arrd.1980.121.6.959

**Delfino RJ, Sioutas C, Malik S**. 2005. Potential role of ultrafine particles in associations between airborne particle mass and cardiovascular health. Environ Health Persp. 113(8):934–946. doi:10.1289/ehp.7938

**Fierz M, Meier D, Steigmeier P, Burtscher H**. 2014. Aerosol measurement by induced currents. Aerosol Sci Technol. 48(4):350–357. doi:10.1080/02786826.2013.875981

**Fissan H, Neumann S, Trampe A, Pui DYH, Shin WG**. 2006. Rationale and principle of an instrument measuring lung deposited nanoparticle surface area. J Nanopart Res. 9(1):53–59. doi:10.1007/978-1-4020-5859-2_6

**Garcia J, Bennett DH, Tancredi D, Schenker MB, Mitchell D, Reynolds SJ, Mitloehner FM**. 2013. Occupational exposure to particulate matter and endotoxin for California dairy workers. Int J Hyg Environ Health. 16(1):56–62. doi:10.1016/j.ijheh.2012.04.001

**Geiss O, Bianchi I, Barrero-Moreno J**. 2016. Lung-deposited surface area concentration measurements in selected occupational and non-occupational environments. J Aerosol Sci. 96:24–37. doi:10.1016/j.jaerosci.2016.02.007

**Higgins IT, Glassman JH, Oh MS, Cornell RG**. 1983. Mortality of reserve mining company employees in relation to taconite dust exposure. Am J Epi. 118(5):710–719. doi:10.1093/oxfordjournals.aje.a113681

**Huynh T, Ramachandran G, Quick H, Hwang J, Raynor PC, Alexander BH, Mandel JH**. 2018. Real-time fine aerosol exposures in taconite mining operations. Ann Work Exp Health. 63(1):77–90. doi:10.1101/263442

**Lin W, Huang Y, Zhou XD, Ma Y**. 2006. In vitro toxicity of silica nanoparticles in human lung cancer cells. Toxicol Appl Pharm. 217(3):252–259. doi:10.1016/j.taap.2006.10.004

**Kuhlbusch TA, Asbach C, Fissan H, Göhler D, Stintz M**. 2011. Nanoparticle exposure at nanotechnology workplaces: A review. Part Fibre Toxicol. 8(1):22. doi:10.1186/1743-8977-8-22

**Kuuluvainen H, Rönkkö T, Järvinen A, Saari S, Karjalainen P, Lähde T, Pirjola L, Niemi JV, Hillamo R, Keskinen J**. 2016. Lung deposited surface area size distributions of particulate matter in different urban areas. Atmos Environ. 136:105–113. doi:10.1016/j.atmosenv.2016.04.019

**McDonald C, Baker-Muhich B, Fitz T, Garrison P, Petchenik J, Rasmussen P, Thiboldeaux R, Walker W, Watras C**. 2013. Taconite Iron Mining in Wisconsin: A Review. Wisconsin Department of Natural Resources, Bureau of Science Services.

**Mills JB, Park JH, Peters TM**. 2013. Comparison of the DiSCmini aerosol monitor to a handheld condensation particle counter and a scanning mobility particle sizer for submicrometer sodium chloride and metal aerosols. J Occup Environ Hyg. 10(5):250–258. doi:10.1080/15459624.2013.769077

**Mitakakis TZ, McGee PA**. 2000. Reliability of measurement of spores of Alternaria and pollen concentrations in air over two towns in rural Australia. Grana 39(2–3):141–145. doi:10.1080/001731300300045300

**Nelson G, Murray J**. 2013. Silicosis at autopsy in platinum mine workers. Occup Med. 63(3):196–202. doi:10.1093/occmed/kqs211

**Nolan R, Langer A, Wilson RA**. 1999. Risk assessment for exposure to grunerite asbestos (Amosite) in an iron ore mine. P Natl Acad Sci USA 96(7):3412–3419. doi:10.1073/pnas.96.7.3412

**O'Shaughnessy PT, Slagley JM**. 2002. Photometer response determination based on aerosol physical characteristics. AIHA J. 63(5):578–585. doi:10.1080/15428110208984743

**Occupational Safety and Health Administration (OSHA)**. OSHA Fact Sheet, https://www.osha.gov/silica/factsheets/OSHA_FS-3683_Silica_Overview.html

**Park JY, Ramachandran G, Raynor PC, Olson GM**. 2010. Determination of particle concentration rankings by spatial mapping of particle surface area, number, and mass concentrations in a restaurant and a die casting plant. J Occup Environ Hyg. 7(8):466–476. doi:10.1080/15459624.2010.485263

**Ramachandran G, Paulsen D, Watts W, Kittelson D**. 2005. Mass, surface area and number metrics in diesel occupational exposure assessment. J Environ Monitor. 7(7):728. doi:10.1039/b503854e

**Schmid O, Möller W, Semmler-Behnke MA, Ferron G, Karg E, Lipka J, Schulz H, Kreyling WG, Stoeger T**. 2009. Dosimetry and toxicology of inhaled ultrafine particles. Biomarkers 14:67–73. doi:10.1080/13547500902965617

**Sheehy JW, McJilton, CE**. 1987. Development of a model to aid in reconstruction of historical silica dust exposures in the taconite industry. Am Ind Hyg Assoc J. 48(11): 914–918. doi:10.1080/15298668791385804

**Schmid O, Stoeger T**. 2016. Surface area is the biologically most effective dose metric for acute nanoparticle toxicity in the lung. J Aerosol Sci. 99:133–143. doi:10.1016/j.jaerosci.2015.12.006

**Shrout PE, Fleiss JL**. 1979. Intraclass correlations: Uses in assessing rater reliability. Psychol Bull. 86(2):420–428. doi:10.1037/0033-2909.86.2.420

**Todea AM, Beckmann S, Kaminski H, Asbach C**. 2015. Accuracy of electrical aerosol sensors measuring lung deposited surface area concentrations. J Aerosol Sci. 89: 95–109. doi:10.1016/j.jaerosci.2015.07.003

**Todea AM, Beckmann S, Kaminski H, Bard D, Bau S, Clavaguera S, Dahmann D, Dozol H, Dziurowitz N, Elihn K, Fierz M**. 2017. Inter-comparison of personal monitors for nanoparticles exposure at workplaces and in the environment. Sci Total Environ. 15(605):929–945. doi:10.1016/j.scitotenv.2017.06.041

**Yu KO, Grabinski CM, Schrand AM, Murdock RC, Wang W, Gu B, Hussain SM**. 2009. Toxicity of amorphous silica nanoparticles in mouse keratinocytes. J Nanopart Res. 11(1):15–24. doi:10.1007/s11051-008-9417-9

**Zellweger C, Huglin C, Klausen J, Steinbacher M, Vollmer M, Buchman B**. 2009. Inter-comparison of four different carbon monoxide measurement techniques and evaluation of the long-term carbon monoxide time series of Jungfraujoch. Atm Chem Phys. 9:3491–3503. doi:10.5194/acp-9-3491-2009